Bioorganic & Medicinal Chemistry Letters 20 (2010) 6899–6904

Contents lists available at ScienceDirect

Bioorganic & Medicinal Chemistry Letters

journal homepage: www.elsevier.com/locate/bmcl

# Interaction of 3′-azido-3′-deamino daunorubicin with human serum albumin: Investigation by fluorescence spectroscopy and molecular modeling methods

Yan Lu [a], Qingqin Feng [c], Fengling Cui [a,*], Weiwei Xing [a], Guisheng Zhang [a,*], Xiaojun Yao [b]

[a] School of Chemistry and Environmental Science, Key Laboratory for Environmental Pollution Control Technology of Henan Province, Henan Normal University, Xinxiang 453007, People's Republic of China
[b] Department of Chemistry, Lanzhou University, Lanzhou 730000, People's Republic of China
[c] School of Chemistry and Chemical Engineering, Anyang Normal University, Anyang 455002, People's Republic of China

ARTICLE INFO

*Article history:*
Received 4 August 2010
Revised 28 September 2010
Accepted 2 October 2010
Available online 27 October 2010

*Keywords:*
3′-Azido-3′-deamino daunorubicin (ADNR)
Human serum albumin (HSA)
Fluorescence quenching
Molecular modeling
Synchronous fluorescence
UV–vis absorption spectrum

ABSTRACT

In this Letter, the binding of 3′-azido-3′-deamino daunorubicin (ADNR) to human serum albumin (HSA) was investigated at different temperatures by fluorescence spectroscopy at pH 7.4. The binding constant was determined according to Stern–Volmer equation based on the fluorescence quenching of HSA in the presence of ADNR. The thermodynamic parameters, $\Delta H$ and $\Delta S$, were calculated according to the dependence of enthalpy change on the temperature to be $-21.01$ kJ mol$^{-1}$ and 24.71 J K$^{-1}$ mol$^{-1}$, respectively. The results revealed that ADNR had a strong ability to quench the intrinsic fluorescence of HSA through a static quenching procedure. The hydrophobic force played a major role in the interaction of ADNR with HSA, which was in good agreement with the results of molecular modeling study. The effect of various metal ions on the binding constants of ADNR with HSA was also investigated. All the experimental results and theoretical data indicated that ADNR could bind to HSA and be effectively transported and eliminated in body, which might be a useful guideline for further drug design.



Anthracyclines, such as daunorubicin and doxorubicin, are considered to be some of the most effective anticancer drugs for cancer therapy. However, drug resistance and cardiotoxicity of anthracyclines limit their clinical application. In our previous research[1], a daunorubicin analogue, 3′-azido-3′-deamino daunorubicin (ADNR, Fig. 1), were synthesized by directly transforming the amino group of daunorubicin to an azido group. ADNR exhibited potent anticancer activity in both drug-sensitive (K562) and drug-resistant leukemia cells (K562/Dox), with a 25-fold lower drug resistance index than parent compound daunorubicin. An in vivo xenograft model demonstrated that ADNR showed more than 2.5-fold higher maximum growth inhibition rate against drug-resistant cancers and significant improvement for animal survival rate versus daunorubicin. No significant body weight reduction in mice was observed for ADNR at the maximum tolerable dose, as compared to more than 70% body weight reduction for daunorubicin.[1] The compound ADNR is worthy of further evaluation as a new drug candidate.

It has been shown that the distribution, free concentration and the metabolism of various drugs may be strongly affected by drug–protein interactions in the blood stream. This type of interaction can also influence the drug stability and toxicity during the chemotherapeutic process. Serum albumins have many physiological functions and play a dominant role in drug disposition and efficacy.[2,3] Many drugs and other small bioactivity molecules bind reversibly to albumin and other serum components that then function as carriers. Consequently, it is important to know the affinity of a drug to serum albumin, even if it is not the only factor to predict serum concentrations of the free drug.

Serum albumins have been the most studied proteins for many years. They are the most abundant protein in blood plasma, accounting for about 60% of the total protein as a concentration of 42 g L$^{-1}$ [4,5] and provide about 80% of the osmotic pressure of blood.[4] Recently, the three-dimensional structure of human serum

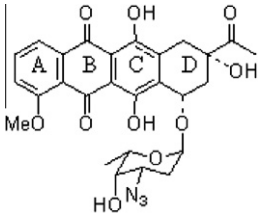


**Fig. 1.** The structure of ADNR.

* Corresponding authors. Tel./fax: +86 373 3326336 (F.C.); tel./fax: +86 373 3325250 (G.Z.).
*E-mail addresses:* fenglingcui@hotmail.com (F. Cui), zgs6668@yahoo.com (G. Zhang).

0960-894X/$ - see front matter © 2010 Elsevier Ltd. All rights reserved.
doi:10.1016/j.bmcl.2010.10.009

albumin (HSA) has been determined through X-ray crystallographic measurements.[2] The globular protein consists of a single polypeptide chain of 585 amino acid residues and has many important physiological functions.[6,7] There are typical sites of coordination for several substances such as amino acids, fatty acids, hormones, and drugs.[5] The multiple binding sites underlie the exceptional ability of HSA to interact with many substances and make this protein an important regulator of intercellular fluxes and pharmacokinetic behavior of many drugs.

In the present work, the binding of ADNR to HSA was studied by using fluorescence, UV–vis absorption spectrum and molecular modeling methods. The nature of drug binding to protein was described. The effect of the energy transfer was studied according to the Förster theory of non-radiation energy transfer.

Appropriate amounts of human serum albumin (Hualan Biological Engineering Limited Company) was directly dissolved in water to prepare stock solution at final concentration of $2.0 \times 10^{-5}$ M and stored in the dark at 0–4 °C. $3.67 \times 10^{-4}$ M ADNR was dissolved in *N*,*N*-dimethylformamide (DMF), 0.5 M NaCl working solution, 0.1 M Tris–HCl buffer solution of pH 7.4 and other ionic solutions were prepared. All chemicals were of analytical reagent grade and were used without further purification. Double distilled water was used throughout.

All fluorescence spectra were recorded on a FP-6200 spectrofluorimeter (JASCO, Japan) and a RF-540 spectrofluorimeter (Shimadzu, Japan) equipped with a thermostat bath, using 5/5 nm slit widths. The UV absorption spectra were performed on a Tu-1810 ultraviolet-visible spectrophotometer (Beijing General Instrument, China). The pH values were measured on a pH 3 digital pH-meter (Shanghai Lei Ci Device Works, Shanghai, China) with a combined glass electrode. All calculations were performed on SGI workstation in the molecular model study.

ADNR was synthesized starting from daunorubicin hydrochloride according to the known method[1] as a red solid in 70% yield: HRMS $(M+Na)^+$ (ESI) calcd for $C_{27}H_{27}N_3O_{10}Na^+$ 576.1589, found 576.1612; $^1$H NMR (500 MHz, $CDCl_3$) 13.95 (1H, s, HO-6), 13.19 (1H, s, HO-11), 7.98 (1H, d, *J* = 7.4 Hz, H-1), 7.74 (1H, t, *J* = 8.2 Hz, H-2), 7.36 (1H, d, *J* = 8.4 Hz, H-3), 5.54 (1H, d, *J* = 3.6 Hz, H-1′), 5.23 (1H, d, *J* = 1.9 Hz, H-7), 4.37 (1H, s, HO-9), 4.10 (1H, m, H-5′), 4.05 (3H, s, MeO-4), 3.69 (1H, br, H-4′), 3.60 (1H, m, H-3′), 3.15 (1H, dd, *J* = 1.6 Hz, *J* = 18.8 Hz, Ha-10), 2.87 (1H, d, *J* = 18.8 Hz, Hb-10), 2.38 (3H, s, H-14), 2.28 (1H, m, Ha-8), 2.09 (2H, m, Hb-8, Ha-2′), 1.91 (1H, m, Hb-2′), 1.30 (3H, d, *J* = 6.6 Hz, H-6′); $^{13}$C NMR (125 MHz, $CDCl_3$) 211.5, 186.9, 186.7, 161.1, 156.3, 155.7, 135.7, 135.5, 134.2, 133.9, 120.8, 119.8, 118.5, 111.5, 111.3, 100.6, 76.7, 70.1, 69.5, 67.1, 56.8, 56.7, 34.9, 33.3, 28.5, 24.7, 16.8.

For the fluorescence measurement, 2.0 mL Tris–HCl buffer solution, 2.0 mL NaCl solution, appropriate amounts of HSA and ADNR were added to 10.0 mL standard flask and diluted to 10.0 mL with double distilled water. Fluorescence quenching spectra of HSA were obtained at excitation wavelength (280 nm) and emission wavelength (300–450 nm). The UV absorption and synchronous fluorescence spectra of the above system were also recorded. In addition, fluorescence spectra in the presence of other ions were measured at the same conditions.

The synchronous fluorescence spectra were obtained by simultaneously scanning the excitation and emission monochromators.[8] When the wavelength interval ($\Delta\lambda$) was fixed at 60 nm, the synchronous fluorescence had the same intensity as the emission fluorescence following excitation at 280 nm, just the emission maximum wavelength and shape of the peaks were changed.[9–11] Thus, the synchronous fluorescence measurements can be applied to calculate association constants similar to the emission fluorescence measurements and deduce the binding mechanism. In this study, the synchronous fluorescence spectra of tyrosine residues and tryptophan residues were measured at $\lambda_{em}$ = 280 nm ($\Delta\lambda$ = 15 and 60 nm) in the absence and in the presence of various amounts of ADNR.

The potential of the 3D structures of HSA was assigned according to the Amber 4.0 force field with Kollman-all-atom charges. The initial structures of all the molecules were generated by molecular modeling software SYBYL 6.9.1. The geometries of this drug were subsequently optimized using the Tripos force field with Gasteiger–Marsili charges. The AutoDock3.05 program was used to calculate the interaction modes between the drug and HSA. Lamarckian genetic algorithm (LGA) implemented in Autodock was applied to calculate the possible conformation of the drug that binds to the protein. During docking process, a maximum of 10 conformers was considered for the drug. The conformer with the lowest binding free energy was used for further analysis. All calculations were performed on SGI FUEL workstation.

It is well known that HSA is a monomeric protein comprising 585 amino acids. And its secondary structure is mainly α-helix and 17 disulfide bridges. The initial crystal structure analyses have revealed that the principal regions of ligand binding sites of albumin are located in hydrophobic cavities in subdomains IIA and IIIA, and the sole tryptophan residue (Trp-214) is in subdomain IIA.[12] Numerous studies confirmed that the binding of small molecule substances to HSA could induce the conformational change of HSA, because the intramolecular forces involved to maintain the secondary structure could be altered, which results in the conformational change of protein.[13–24] Actually, the intrinsic fluorescence of HSA is almost contributed by tryptophan alone.[25] The change of intrinsic fluorescence intensity of HSA is that of fluorescence intensity of tryptophan residue when small molecule substances are added to HSA. The fluorescence quenching spectra of HSA at various concentrations of ADNR are shown in Figure 2. Obviously, HSA had a strong fluorescence emission band at 342 nm by fixing the excitation wavelength at 280 nm, while ADNR had no intrinsic fluorescence. The fluorescence intensity of HSA decreased regularly, and slight blue shift was observed for the emission wavelength with increasing ADNR concentration. Therefore, we inferred that the binding took place near Trp-214 and led to a conformational change with a local perturbation of the IIA binding site in HSA.

The synchronous fluorescence spectra present the information about the molecular microenvironment in the vicinity of the fluorophore functional groups. In the synchronous fluorescence of HSA, the shift in position of maximum emission wavelength corresponds to the changes of polarity around the fluorophore of amino acid residues. The $\Delta\lambda$ values (scanning interval, $\Delta\lambda = \lambda_{em} - \lambda_{ex}$)

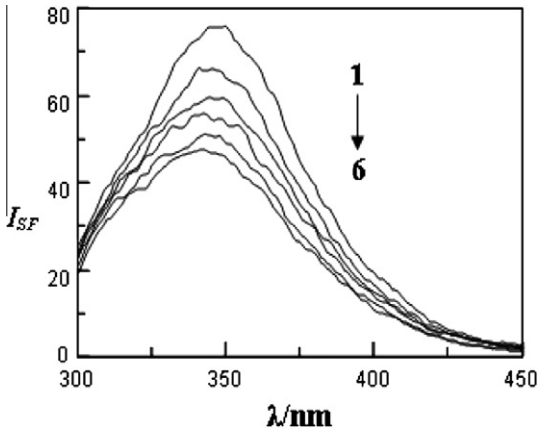


**Fig. 2.** The fluorescence spectra of ADNR–HSA system. From 1 to 6: $C_{HSA} = 8.0 \times 10^{-7}$ M; $C_{ADNR}$ = 0, 1.8, 3.6, 5.4, 7.2, 9.0 $\times 10^{-6}$ M.

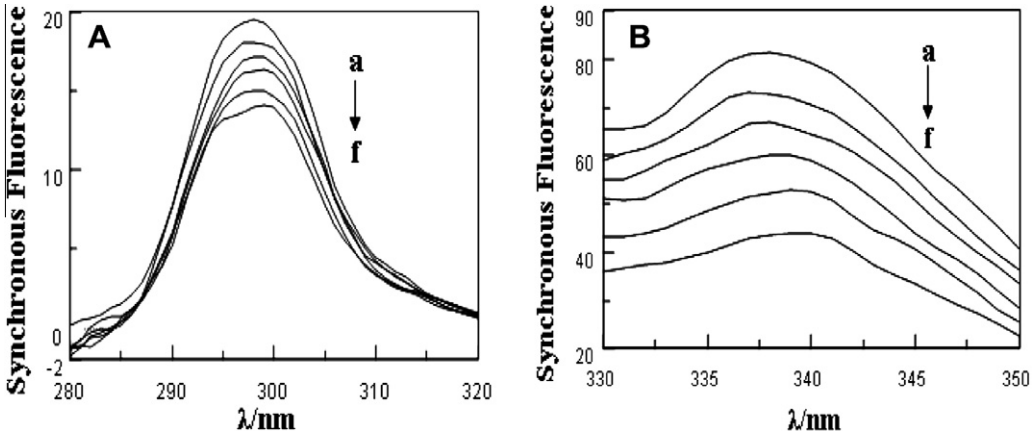


**Fig. 3.** Synchronous fluorescence spectrum of HSA ($T$ = 290 K, pH 7.40), $C_{HSA} = 8\times10^{-7}$ M, c(ADNR)/($10^{-6}$ M), a–f: 0, 1.7, 3.4, 5.1, 6.8, 8.5, A: $\Delta\lambda$ = 15; B: $\Delta\lambda$ = 60 nm.

stabilized at 15 or 60 nm, synchronous fluorescence of HSA gives the characteristic information of tyrosine residues and tryptophan residues, respectively.[26] As can be seen from Figure 3, the fluorescence of tyrosine residues was weak and the position of maximum emission wavelength had little change when $\Delta\lambda$ was 15 nm. While the fluorescence of tryptophan residues was strong and the maximum emission wavelength moderately shifted toward long wave when $\Delta\lambda$ was 60 nm. This reflects the fact that the microenvironment of the tryptophan residue was significantly affected by ADNR binding. It is reported that the maximum emission wavelength ($\lambda_{max}$) at 330–332 nm indicates that tryptophan resides are located in the nonpolar region, namely, they are buried in a hydrophobic cavity of HSA; $\lambda_{max}$ at 350–352 nm shows that tryptophan residues are exposed to water, namely, the hydrophobic cavity in HSA is disagglomerated and the structure of HSA is looser. The red shift effect suggested that ADNR bound to the hydrophobic cavity of HSA resulted in the loose structure of HSA and the polarity around the tryptophan residues was increased while the hydrophobicity was decreased.[27]

UV absorption spectra of ADNR, HSA and ADNR–HSA systems were recorded and shown in Figure 4. The UV absorption intensity of HSA increased with the variation of concentration of ADNR. Furthermore, a slight blue shift of maximum peak position was noticed which might because of the formation of a complex between ADNR and HSA.[28] This also indicated that the peptide strands of protein molecules extended upon the addition of ADNR to HSA.[10]

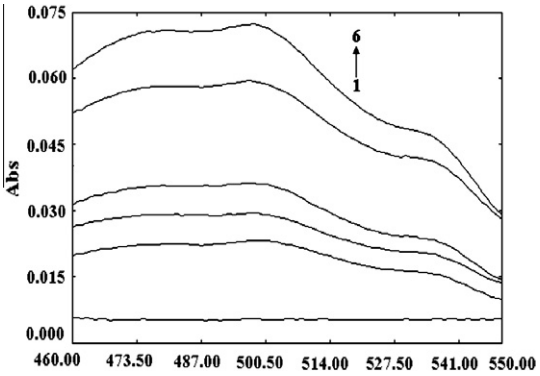


**Fig. 4.** UV absorption spectra of HSA in the absence and presence of ADNR. (1) The UV absorption of HSA, $C_{HSA} = 8\times10^{-7}$ M. (2) The UV absorption of ADNR, $C_{ADNR} = 1.84\times10^{-6}$ M. (3–6) The UV absorption of ADNR–HSA, $C_{HSA} = 8\times10^{-7}$ M; $C_{ADNR} = 1.84\times10^{-6}$ M; $C_{ADNR} = 3.68\times10^{-6}$ M; $C_{ADNR} = 5.52\times10^{-6}$ M; $C_{ADNR} = 7.36\times10^{-6}$ M.

Fluorescence quenching refers to any process which decreases the fluorescence intensity of a sample. It is divided into dynamic quenching or static quenching. Dynamic quenching depends upon diffusion. Since higher temperatures result in larger diffusion coefficients, the bimolecular quenching constants are expected to increase with increasing temperature. In contrast, increased temperature is likely to result in decreasing stability of complexes, and thus lower values of the static quenching constants.

In order to speculate the fluorescence quenching mechanism, the fluorescence quenching data at different temperatures (290, 300, and 310 K, Fig. 5) were firstly analyzed using the classical Stern–Volmer equation[29]:

$$F_0/F = 1 + k_q\tau_0[Q] = 1 + K_{SV}[Q] \quad (1)$$

where $F_0$ and $F$ are the fluorescence intensities in the absence and presence of quencher, respectively, $k_q$ the biomolecular quenching constant, $\tau_0$ the life time of the fluorescence in absence of quencher, [$Q$] the concentration of quencher, and $K_{SV}$ is the Stern–Volmer quenching constant. The results summarized in Table 1 showed that the Stern–Volmer quenching constant $K_{SV}$ is inversely correlated with temperature and the values of $k_q$ is larger than the limiting diffusion constant $K_{dif}$ of the biomolecule ($K_{dif} = 2.0\times10^{10}$ $M^{-1}$ $s^{-1}$)[30], which suggested that the fluorescence quenching was caused by a specific interaction between HSA and ADNR, and the quenching

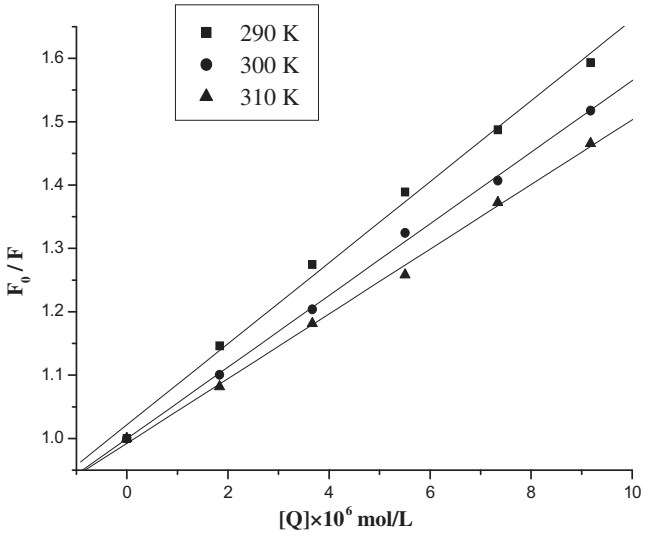


**Fig. 5.** The Stern–Volmer curves for quenching of ADNR with HSA.

**Table 1**
The dynamic quenching constants (L/mol/s) between ADNR and HSA

| $T$ (K) | Stern–Volmer equation | $k_q$ (L/mol/s) | $R$ |
|---|---|---|---|
| 290 | $Y = 1.0218 + 6.392 \times 10^4$ [Q] | $6.392 \times 10^{12}$ | 0.9973 |
| 300 | $Y = 0.9997 + 5.651 \times 10^4$ [Q] | $5.651 \times 10^{12}$ | 0.9993 |
| 310 | $Y = 0.9925 + 5.105 \times 10^4$ [Q] | $5.105 \times 10^{12}$ | 0.9988 |

**Table 2**
The binding constant ($K$/$M$) between ADNR and HSA

| $T$ (K) | Scatchard equation | $K$ (L/mol) | $n$ | $R$ |
|---|---|---|---|---|
| 290 | $Y = 0.0845 - 0.1195r$ | $1.19 \times 10^5$ | 0.7071 | 0.9991 |
| 300 | $Y = 0.0729 - 0.0890r$ | $8.90 \times 10^4$ | 0.8191 | 0.9956 |
| 310 | $Y = 0.0683 - 0.0647r$ | $6.47 \times 10^4$ | 1.0556 | 0.9915 |

was mainly arisen from the predominant of complexes formation, while dynamic collision could be negligible in the concentration studied.[31] Therefore, the quenching data were analyzed according to the Scatchard equation[32]:

$$r/D_f = nK - rK \quad (2)$$

Where $r$ is the number of mol of bound drug per mol of protein, $D_f$ is the concentration of unbound drug, $K$ is the binding constant, and $n$ is the number of binding sites. Figure 6 shows the Scatchard plots for the ADNR–HSA system at different temperatures. The linearity of the Scatchard plot indicated that ADNR bound to a single class of binding sites on HSA and there was a strong interaction between ADNR and HSA (Table 2). The binding constant decreased slightly with the increasing temperature, resulting in a reduction of the stability of the ADNR–HSA complex.

In general, small molecules are bound to the macromolecule by four binding modes: H-bonds, van der Waals, electrostatic and hydrophobic interactions. The thermodynamic parameters, enthalpy ($\Delta H$) and entropy ($\Delta S$) of reaction, are important for confirming the binding mode. From the temperature dependence of binding constants, it is possible to calculate values for the thermodynamic functions involved in the binding process. The binding constants of ADNR to HSA at the three temperatures were estimated. Afterward, the thermodynamic parameters were determined from a linear van't Hoff plot by plotting the binding constants according to van't Hoff equation (Fig. 7) and are presented in Table 3. The corresponding values of $\Delta G$ for three temperatures were also calculated from the relation $\Delta G = \Delta H - T\Delta S$. Nemethy and Scheraga[33], Timasheff[34], Ross and Subramanian[35] characterized the sign and magnitude of the thermodynamic parameter associated with various individual kinds of interaction that might take place in the protein association processes, as described below. $\Delta H > 0$ and $\Delta S > 0$ implies a hydrophobic interaction; $\Delta H < 0$ and $\Delta S < 0$ reflects the van der Waals force or hydrogen bond formation; and $\Delta H \approx 0$ and $\Delta S > 0$ suggests an electrostatic force. Therefore, the binding of ADNR to HSA might involve strongly hydrophobic interaction as verified by the positive

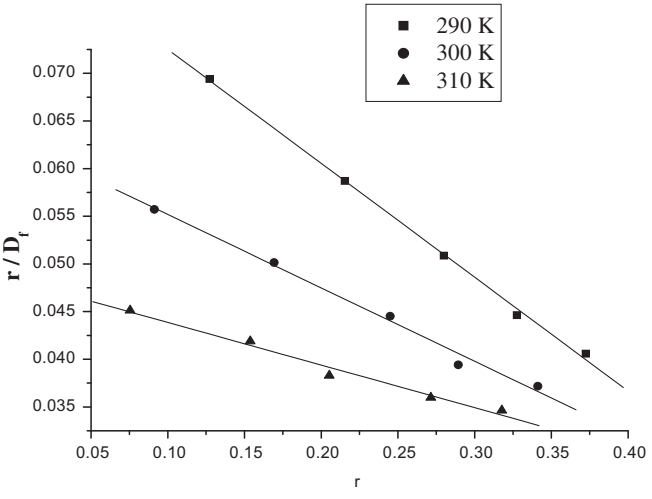


**Fig. 6.** Scatchard plot for the ADNR–HSA.

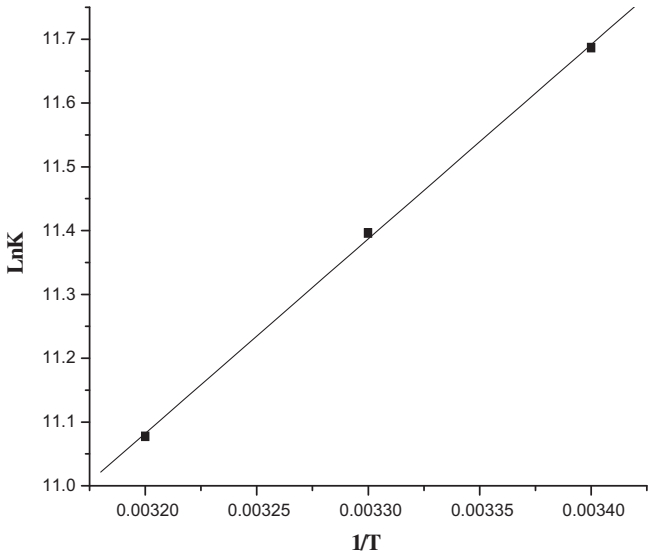


**Fig. 7.** Van't Hoff plot for the interaction of ADNR and HSA.

**Table 3**
The thermodynamic parameters for the binding ADNR to HSA

| $T$ (K) | $\Delta G$ (kJ/mol) | $\Delta H$ (kJ/mol) | $\Delta S$ (J/mol/K) |
|---|---|---|---|
| 290 | −28.18 | | |
| 300 | −28.42 | −21.01 | 24.71 |
| 310 | −28.55 | | |

values of $\Delta S$ while the electrostatic interaction could not be excluded. That is, ADNR bound to HSA was mainly based on the hydrophobic and electrostatic interactions.

The efficiency of energy transfer was studied according to the Förster energy transfer theory.[36] The efficiency of energy transfer, $E$, is described by the following equation:

$$E = 1 - F/F_0 = R_0^6/(R_0^6 + r^6) \quad (3)$$

where $F$ and $F_0$ are the fluorescence intensities of HSA in the presence and absence of ADNR, $r$ the distance between acceptor and donor, and $R_0$ the critical distance when the transfer efficiency is 50%:

$$R_0^6 = 8.8 \times 10^{-25} k^2 n^{-4} \Phi J \quad (4)$$

where $K^2$ is the spatial orientation factor of the dipole, $N$ the refractive index of the medium, $\Phi$ the fluorescence quantum yield of the donor, $J$ the overlap integral of the fluorescence emission spectrum of the donor and the absorption spectrum of the acceptor. $J$ is given by

$$J = \sum F(\lambda)\varepsilon(\lambda)\lambda^4 \Delta\lambda / \sum F(\lambda)\Delta\lambda \quad (5)$$

where $F(\lambda)$ is the fluorescence intensity of the fluorescent donor at wavelength $\lambda$, $\varepsilon(\lambda)$ is the molar absorption coefficient of the acceptor at wavelength $\lambda$. From the above relationships, $J$ and $E$ can be easily obtained; therefore, $R_0$ and $r$ can be further calculated. Figure 8 shows the overlap of the fluorescence spectrum of

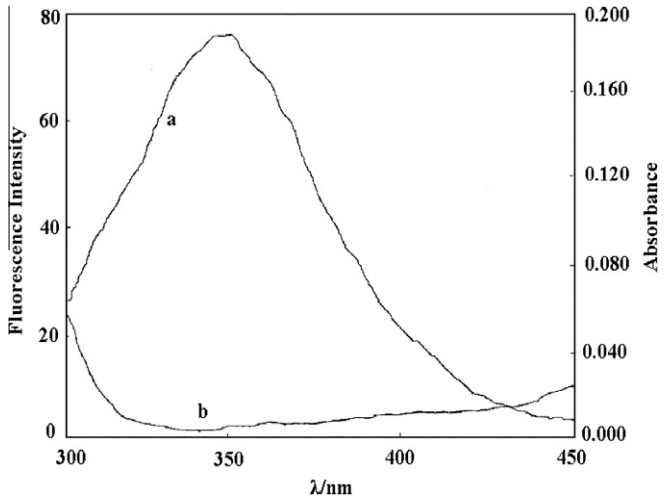


**Fig. 8.** The overlap of UV absorption spectrum of ADNR with the fluorescence emission spectrum of HSA. (a) The fluorescence emission spectrum of HSA ($8 \times 10^{-7}$ M); (b) the UV absorption spectrum of ADNR ($1.7 \times 10^{-6}$ M).

HSA and the absorption spectrum of ADNR. $J$ was obtained to be $1.471 \times 10^{-14}$ cm$^3$ M$^{-1}$ by integrating the overlap of the UV absorption spectrum of ADNR and the fluorescence emission spectrum of HSA, and $E$ was calculated to be 0.2386. It was reported earlier that $K^2 = 2/3$, $\Phi = 0.118$, $n = 1.336$ for HSA.[37] Based on these data, it could be found that $R_0 = 2.6$ nm and $r = 3.58$ nm. The distance between ADNR and tryptophan residue in HSA 3.58 nm was far lower than 7 nm. These were in accordance with conditions of Förster energy transfer theory.

HSA has a limited number of binding sites for endogenous and exogenous ligands that are typically bound reversibly and have binding constants in the range of $10^4$–$10^8$ M$^{-1}$.[38] The principal regions of ligand binding sites of albumin are located in hydrophobic cavities in subdomains IIA and IIIA, which exhibit similar chemistry. To explore which binding site of HSA that ADNR was located, the complementary applications of molecule modeling were employed to improve the understanding of the interaction between HSA and ADNR. The crystal structure of HSA in complex with R-warfarin was taken from the Brookhaven Protein Data Bank (entry codes 1h9z).[39] Figure 9 shows the best energy ranked results, ADNR molecule was located within the binding pocket of subdomain IIA and the A, B, C, and D rings were practically coplanar. Site I was large enough to accommodate the ADNR molecule. It was important to note that the residues of HSA, ALA215, and HIS288 were in close proximity to the ADNR, suggesting the existence of hydrophobic interaction between them. In addition there were also a number of specific electrostatic interactions and hydrogen because several ionic and polar residues in the proximity of the ligand played an important role in stabilizing the negatively charged ADNR molecule via H-bonds and electrostatic interaction. The residue ALA215 of HSA was suitable position to form intermolecular H-bond. Additionally, HIS288, HIS242, and LYS286 from the IIA subdomain were able to form intermolecular H-bond with E-ring. The results indicated that the formation of hydrogen bond decreased the hydrophilicity and increased the hydrophobicity to keep stability in the ADNR–HSA system. The amino acid residues with a benzene ring could match ADNR in space to firm the conformation of the complex. The results obtained from modeling indicated that the interaction between ADNR and HSA was dominated by a hydrophobic force, and there were also electrostatic interaction, hydrogen bonds between the drug and the polar amino acid residues. It is important to note that the Trp-214 residue of HSA was in close proximity to the C-ring, this finding provided a good structural basis to explain the efficient fluorescence quenching of HSA emission in the presence of ADNR.[23]

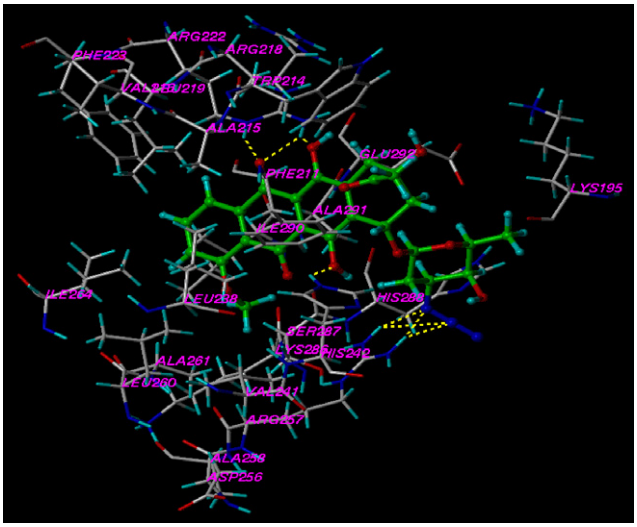


**Fig. 9.** The interaction model between ADNR and HSA. The residues of ADNR and HSA are represented using different tinctorial stick model. The hydrogen bond between the ligand and the protein is indicated by dashed line.

The previous studies indicated that HSA had a high affinity metal-binding site at N-terminus. The multiple binding sites underlay the exceptional ability of HSA to interact with many organic and inorganic molecules and made this protein an important regulator of intercellular fluxes and the pharmacokinetic behavior of many drugs.[5] The common ions are widely distributed in human and animals. Therefore, it was of interest to examine the effect of inorganic cations and anions in the solution system of ADNR–HSA. Table 4 displays the results of the effect of common ions on the binding constants at 290 K. The binding constants between HSA and ADNR decreased from 5.88% to 79.83% in the presence of common ions. As a result, the binding force between protein and pharmaceutical also decreased, shortened the stored time of pharmaceutical in blood plasma and improved maximum reaction intensity of pharmaceutical.

A fluorescence method for the rapid and simple determination of the interaction between HSA and ADNR was provided. The method was reliable, practical, and easy to operate. The results obtained gave preliminary information on the binding of ADNR to HSA. The hydrophobic interaction played a major role in stabilizing the complex. The distance between HSA and ADNR was 3.58 nm according to fluorescence resonance energy transfer. The results of synchronous fluorescence and UV–vis absorption spectroscopy indicated that the conformation of HSA was changed in the presence of ADNR.

The study of binding drugs to protein is of great importance in pharmacy, pharmacology and biochemistry. This study was

**Table 4**
The binding constants between ADNR and HSA in the presence of other ions

| Ions | $K$ ($\times 10^4$) | $R$ | Ions | $K$ ($\times 10^4$) | $R$ |
|---|---|---|---|---|---|
| $Na^+$ | 11.12 | 0.9980 | $Ni^{2+}$ | 6.30 | 0.9983 |
| $Co^{2+}$ | 6.34 | 0.9997 | $Cd^{2+}$ | 6.33 | 0.9984 |
| $F^-$ | 6.18 | 0.9996 | $Bi^{3+}$ | 8.10 | 0.9982 |
| $PO_4^{3-}$ | 4.77 | 0.9979 | $NH_4^+$ | 10.71 | 0.9981 |
| $Pb^{2+}$ | 7.85 | 0.9998 | $K^+$ | 8.71 | 0.9999 |
| $CO_3^{2-}$ | 11.02 | 0.9989 | $Al^{3+}$ | 2.40 | 0.9992 |
| $Mg^{2+}$ | 5.84 | 0.9996 | $Hg^{2+}$ | 11.2 | 0.9988 |
| $SO_4^{2-}$ | 8.08 | 0.9999 | $C_2O_4^{2-}$ | 6.49 | 0.9982 |

expected to provide important insight into the interactions of the physiologically important protein HSA with the new drug ADNR. Information about the effect of environment on HSA structure was also obtained which might be correlated to its physiologically activity.

## Acknowledgments

This work was supported by the National Natural Science Foundation of China (30970696, 20872029) and Innovation Scientists and Technicians Troop Construction Projects of Henan Province (084100510002) to G.Z.

## References and notes

1. Fang, L.; Zhang, G.; Li, C.; Zheng, X.; Zhu, L.; Xiao, J. J.; Szakacs, G.; Nadas, J.; Chan, K. K.; Wang, P. G.; Sun, D. *J. Med. Chem.* **2006**, *49*, 932.
2. He, X. M.; Carter, D. C. *Nature* **1992**, *258*, 209.
3. Olson, R. E.; Christ, D. D. *Annu. Rep. Med. Chem.* **1996**, *31*, 327.
4. Brown, J. R.; Shockley, P. In *Lipid–Protein Interactions*; Wiley: New York, 1982.
5. Carter, D.; Ho, J. X. *Adv. Protein Chem.* **1994**, *45*, 153.
6. Yamasaki, K.; Maruyama, T.; Kragh-Hansen, U.; Otagiri, M. *Biochim. Biophys. Acta* **1996**, *1295*, 147.
7. Carter, D. C.; He, X. M.; Munson, S. H.; Twigg, P. D.; Gernert, K. M.; Broom, M. B.; Miller, T. Y. *Science* **1989**, *244*, 1195.
8. Rubio, S. A.; Gomez-Hens, A.; Ualcarcel, M. *Talanta* **1986**, *33*, 633.
9. Li, D. J.; Zhu, J. F.; Jin, J.; Yao, X. J. *J. Mol. Struct.* **2007**, *846*, 34.
10. Hua, Y. J.; Liu, Y.; Wang, J. B.; Xiao, X. H.; Qu, S. S. *J. Pharm. Biomed. Anal.* **2004**, *36*, 915.
11. Wang, Y. Q.; Zhang, H. M.; Zhang, G. C.; Tao, W. H.; Tang, S. H. *J. Mol. Struct.* **2007**, *830*, 40.
12. Sulkowska, A. *J. Mol. Struct.* **2002**, *614*, 227.
13. Chadborn, N.; Bryant, J.; Bain, A. J.; Shea, P. O. *Biophys. J.* **1999**, *76*, 2198.
14. Liu, J. Q.; Tian, J. N.; Zhang, J. Y.; Hu, Z. D.; Chen, X. G. *Anal. Biochem.* **2003**, *376*, 864.
15. Tian, J. N.; Liu, J. Q.; Zhang, J. Y.; Hu, Z. D.; Chen, X. G. *Chem. Pharm. Bull.* **2003**, *51*, 579.
16. Royer, R. E.; David, L.; Jagt, V. *FEBS Lett.* **1983**, *157*, 28.
17. Thomas, E. B.; Bertil, H.; Björn, L. *FEBS Lett.* **1978**, *86*, 25.
18. Bishop, E. O.; Kimber, S. J.; Smith, B. E.; Beynon, P. J. *FEBS Lett.* **1979**, *101*, 31.
19. Cui, F. L.; Fan, J.; Ma, D. L.; Liu, M. C.; Chen, X. G.; Hu, Z. D. *Anal. Lett.* **2003**, *36*, 2151.
20. Nahar, S.; Carpentier, R.; Tajmir-Riahi, H. A. *J. Inorg. Biochem.* **1997**, *65*, 245.
21. Filyasova, A. I.; Kudelina, I. A.; Feofanov, A. V. *J. Mol. Struct.* **2001**, *565–566*, 173.
22. Bertucci, C.; Ascoli, G.; Barretta, G. U.; Bari, L. D.; Salvadori, P. *J. Pharm. Biomed. Anal.* **1995**, *13*, 1087.
23. Zsila, F.; Bikádi, Z.; Simonyi, M. *Biochem. Pharmacol.* **2003**, *65*, 447.
24. Jiang, C. Q.; Gao, M. X.; Meng, X. Z. *Spectrochim. Acta, Part A* **2003**, *59*, 1605.
25. Colmenarejo, G. *Med. Res. Rev.* **2003**, *23*, 275.
26. Miller, J. N. *Anal. Proc.* **1979**, *16*, 203.
27. He, W. Y.; Li, Y.; Tian, J. N.; Liu, H. X.; Hu, Z. D.; Chen, X. G. *J. Photochem. Photobiol., A* **2005**, *174*, 53.
28. Cui, F. L.; Fan, J.; Li, J. P.; Hu, Z. D. *Bioorg. Med. Chem.* **2004**, *12*, 151.
29. Eftink, M. R. Fluorescence Quenching Reactions: Probing Biological Macromolecular Structures. In *Biophysical and Biochemical Aspects of Fluorescence Spectroscopy*; Dewey, T. G., Ed.; Plenum Press: New York, 1991.
30. Lakowica, J. R.; Weber, G. *Biochemistry* **1973**, *12*, 4161.
31. Yang, M. M.; Yang, P.; Zhang, L. W. *Chin. Sci. Bull.* **1994**, *39*, 734.
32. Hu, Y. J.; Liu, Y.; Pi, Z. B.; Qu, S. S. *Bioorg. Med. Chem.* **2005**, *13*, 6609.
33. Nemethy, G.; Scheraga, H. A. *J. Phys. Chem.* **1962**, *66*, 1773.
34. Timasheff, S. N. Thermodynamic of Protein Interactions [M]. In *Proteins of Biological Fluids*; Peeters, H., Ed.; Pergamon Press: Oxford, 1972; pp 511–519.
35. Ross, P. D.; Subramanian, S. *Biochemistry* **1981**, *20*, 3096.
36. Förster, T.. In *Modern Quantum Chemistry*; Sinanoglu, O., Ed.; Academic Press: New York, 1996; Vol. 3,.
37. Cui, F. L.; Qin, L. X.; Zhang, G. S.; Yao, X. J.; Du, J. *Int. J. Biol. Macromol.* **2008**, *42*, 221.
38. Peters, J. A. In *All About Albumin: Biochemistry Genetics and Medical Applications [M]*; Academic Press: San Diego, 1996.
39. Petitpas, I.; Bhattacharya, A. A.; Twine, S.; East, M.; Curry, S. *J. Biol. Chem.* **2001**, *276*, 22804.